Probability of Outage Due to Self-Interference in Indoor Wireless Environments

Indrakshi Dey, *Member, IEEE*, and P. Salvo Rossi, *Senior Member, IEEE*

***Abstract*— In this letter, we derive a mathematically tractable expression for the outage probability in the presence of self-interference over indoor wireless environments modeled through the recently proposed joint fading and two-path shadowing channel model. The effect of self-interference is studied under two different conditions encountered in single-frequency network architectures: 1) long propagation delay and correlated shadow fading in a densely deployed single access point to single mobile user communication scenario and 2) interference between radiated and received signal power in full-duplex radios equipped with multiple antennas both for transmission and reception of data. The analysis is validated numerically both for single-channel and multiple-channel receivers.**

***Index Terms*— Outage probability, joint fading/shadowing channel, indoor radio propagation, performance analysis.**

I. Introduction

INTERFERENCE, between the signal components transmitted over any wireless link and their own distorted and delayed versions, arises at the receiver due to correlated shadow fading and long-delayed paths of the original signal. The reflected and delayed versions of the principal signal components contribute to multipath fading, while the distorted and down-scaled versions of the non-principal signal components give rise to *self-interference* [1], [2]. The amount of self-interference becomes substantial if the propagation delay from a far-away transmitter (relative to nearby transmitters) exceeds a certain threshold.

Self-interference is a common occurrence in indoor WLANs with densely-deployed access points, where mobile users undergo asymmetric propagation scenarios where some access points are significantly farther than others. As a result, multicarrier systems like CDMA operating over single frequency network (SFN) architecture [3], will suffer from self-interference due to long propagation delay and low transmit power contributed by far-away access points.

Evolution of fifth generation (5G) wireless communications towards denser heterogeneous networks requires high throughput services and low-latency applications which motivates the need for full-duplex radios. Imperfect electromagnetic isolation between the transmitter and the receiver in a full-duplex radio also generates unwanted self-interference [4], which may be severe in indoor scenario [5].

In an indoor wireless environment, the path between the access point and the users is too short for shadowing to be accurately characterized by the log-normal distribution and the mobile users restrict their movement within a small area due to the incapability of most WLAN standards to handle soft hand-offs efficiently over multicarrier systems. Moreover, traditional fading channel models like Rayleigh, Rician, or Nakagami-*m* do not accurately characterize indoor WLANs, since indoor wireless links are subject to both fading and shadowing effects. However, the *joint fading and two-path shadowing (JFTS)* channel model proposed in [6] is shown to be accurate in characterizing such an indoor propagation scenario based on an extensive measurement campaign.

The primary contributions of this letter is to derive mathematically-tractable expression for outage probability in a JFTS fading/shadowing channel with self-interference. Towards this end, we obtain the PDF of the difference of two correlated squared JFTS variates, each representing the desired and self-interfering signals obtained from a full-duplex radio system operating over a SFN. Finally simulation results are used to corroborate this analysis both for single-input-single-output (SISO) and multiple-input-multiple-output (MIMO) systems. Performance analysis over SISO systems evaluates the effect of self-interference due to propagation delay from farther access points relative to nearer ones, while that over MIMO systems quantifies self-interference effects due to improper isolation between radiated and received signal power in full-duplex radios. Both analytic and simulation results revealed that outage probability over a JFTS channel increases with correlation between desired and interfering signals, a trend opposite to traditional fading (like Rayleigh, Nakagami) channel models.

II. System Model

We consider a small cell full-duplex wireless communication system over a JFTS fading/shadowing channel in an indoor wireless environment. It employs a full-duplex base station (BS) equipped with M_T transmit antennas for data transmission in the downlink channels and M_R receive antennas for receiving data over the uplink channels at the same time over the same frequency band. Under these conditions, the radiated power over the downlink channels interfere with its own desired received signals over the uplink channels resulting in self-interference at the receiver.[1] Let the instantaneous desired signal power at the receive end of the BS is denoted by $S_D \triangleq \sum_{r=1}^{M_R} S_{D,r} = M_R S_{D,r}$ and the instantaneous

[1]It is to be mentioned here, that in-band full-duplex radios can be implemented using multiple circulators equipped with multiple shared antennas [9]. But this kind of design suffers from severe co-channel interference (CCI) among the shared antennas. The other option is to use physically separate antenna groups for transmission and reception [10]. This kind of design minimizes CCI at the cost of loss in spatial degree of freedom. We consider the later case for our analysis as it is only plagued with inherent self-interference rather than a combination of CCI and self-interference observed in the first case.

Manuscript received August 27, 2016; accepted September 20, 2016. Date of publication September 27, 2016; date of current version January 6, 2017. This work was supported in part by the ERCIM (European Research Consortium for Informatics and Mathematics) within the Alain Bensoussan Fellowship Program. The associate editor coordinating the review of this letter and approving it for publication was C.-H. Lee.

The authors are with the Department of Electronics and Telecommunications, Norwegian University of Science and Technology, 7491 Trondheim, Norway (e-mail : indrakshi.dey@ntnu.no; salvorossi@ieee.org).

Digital Object Identifier 10.1109/LCOMM.2016.2613979

interfering signal power by $S_I \triangleq \sum_{t=1}^{M_T} S_{I,t} = M_T S_{I,t}$. If the variance of the total additive white Gaussian noise (AWGN) inflicting the receiver is given by N, the instantaneous signal-to-interference-plus-noise ratio (SINR) can be defined as, $\nu \triangleq \frac{S_D}{S_I+N}$. Due to shadowing over a broad angle spread and long-delayed paths of the signal in multipath fading, S_D and S_I are correlated with correlation coefficient $\rho = \frac{\mathrm{Cov}(S_D,S_I)}{\sqrt{\mathrm{Var}(S_D)\mathrm{Var}(S_I)}}$, where $\mathrm{Cov}(\cdot)$ and $\mathrm{Var}(\cdot)$ denote covariance and variance, respectively.

A. JFTS Distribution

Let $\mathcal{J}(K, \sigma, \Delta, P_1, P_2)$ represent the JFTS-distributed random variable with fading parameter K (ratio of the specular power to the diffused power contributed by multiple reflections due to individual scatterers within a scattering cluster), shadowing parameter σ (range of shadowing values experienced across different scattering clusters), and shape parameters Δ (ratio of the magnitudes of the shadowing values contributed by two consecutive scattering clusters), P_1 and P_2 (mean-squared values of the diffused and shadowed components, respectively). The PDF of a JFTS-distributed random variable A is given by [6],

$$f_A(\alpha) = \sum_{j=1}^{4} \frac{b_j \alpha}{2P_1P_2} \sum_{h=1}^{m} R_h\, e^{-K-\sigma-\frac{\alpha^2}{2P_2 r_h^2}} \times \Big[e^{B_j} I_0\big(2\alpha\sqrt{\xi_{1j}}\big) + e^{-B_j} I_0\big(2\alpha\sqrt{\xi_{2j}}\big)\Big] \quad (1)$$

where $B_j = \sigma\Delta T_j$, $\xi_{1j} = K\sigma(1-\Delta T_j)/(P_1P_2)$, $\xi_{2j} = K\sigma(1+\Delta T_j)/(P_1P_2)$, $R_h = \frac{\omega_h}{|r_h|} e^{r_h^2 - \frac{r_h^2}{2P_1}}$, I_0 is the 0th-order modified Bessel function of the first kind, $T_j = \cos((j-1)\pi/7)$, $\omega_h = (2^{m-1}m!\sqrt{\pi})/(m^2[H_{m-1}(r_h)]^2)$ are the Gauss-Hermite quadrature weight factors, r_h's are the roots of the Gauss-Hermite polynomial $H_{m-1}(\cdot)$ for $h = 1, 2, \ldots, m$ and m is the approximation index. In (1), $b_j = a_j I_0(1)$, where $a_1 = \frac{751}{17280}$, $a_2 = \frac{3577}{17280}$, $a_3 = \frac{49}{640}$, and $a_4 = \frac{2989}{17280}$. The corresponding nth moment of $f_A(\alpha)$ is given by [7],

$$E\{A^n\} = (4P_1P_2)^{\frac{n}{2}} L_{\frac{n}{2}}(-K) \sum_{j=1}^{4} a_j G^{(n)}(\sigma, \Delta T_j) \quad (2)$$

where, $L_b(\cdot)$ is the Laguerre polynomial and $G^{(n)}(\lambda, \beta) = L_{n/2}(-(1-\beta)\lambda) + L_{n/2}(-(1+\beta)\lambda)$. The PDF of a squared JFTS distributed random variable, $Z = A^2$, can be derived using the procedures for deducing bivariate and joint distributions [8]. The PDF of Z can be expressed as,

$$f_Z(z) = \sum_{j=1}^{4} \frac{b_j}{4P_1P_2} \sum_{h=1}^{m} R_h\, e^{-K-\sigma-\frac{z}{2P_2 r_h^2}} \times \Big[e^{B_j} I_0\big(2\sqrt{z\xi_{1j}}\big) + e^{-B_j} I_0\big(2\sqrt{z\xi_{2j}}\big)\Big] \quad (3)$$

and its corresponding mean can be calculated using the second moment of A, i.e. by putting $n = 2$ in (2), $E\{A^2\} = E\{Z\} = \bar{z} = 4P_1P_2(K+1)(1+\sigma)$. Equivalently, we can write, $P_1P_2 = \bar{z}/(4\hat{K}\hat{\sigma})$, where, $\hat{K} = 1 + K$ and $\hat{\sigma} = 1 + \sigma$. Consequently, the PDF of Z can be written as,

$$f_Z(z) = \sum_{j=1}^{4} \frac{b_j \hat{K}\hat{\sigma}}{\bar{z}} \sum_{h=1}^{m} R_h\, e^{-K-\sigma-\frac{z}{2P_2 r_h^2}} \times \Big[e^{B_j} I_0\Big(4\sqrt{z\hat{\xi}_{1j}}\Big) + e^{-B_j} I_0\Big(4\sqrt{z\hat{\xi}_{2j}}\Big)\Big] \quad (4)$$

where $\hat{\xi}_{1j} = K\sigma\hat{K}\hat{\sigma}(1-\Delta T_j)/\bar{z}$ and $\hat{\xi}_{2j} = K\sigma\hat{K}\hat{\sigma}(1+\Delta T_j)/\bar{z}$.

B. Signal Model

The signal powers of the desired and interfering signals are distributed as,

$$f_{S_D}(s_d) = (1/M_R) \times f_{S_{D,r}}(s_d/M_R) \quad (5)$$

and,

$$f_{S_I}(s_i) = (1/M_T) \times f_{S_{I,t}}(s_i/M_T) \quad (6)$$

respectively. In (5) and (6), $S_{D,r} \sim \mathcal{J}^2(K_D, \sigma_D, \Delta, P_1, P_2)$ and $S_{I,t} \sim \mathcal{J}^2(K_I, \sigma_I, \Delta, P_1, P_2)$, where $\mathcal{J}^2(\cdot)$ denotes squared JFTS distribution, and $S_{D,r}$ and $S_{I,t}$ are assumed to have common shape parameters (Δ, P_1, P_2) and different fading and shadowing parameters (denoted by (K_D, σ_D) and (K_I, σ_I), respectively. The PDF of $S_{D,r}$ and $S_{I,t}$ can be given by (4) with $(K, \sigma, \bar{z}) = (K_D, \sigma_D, \bar{s}_d)$ and $(K, \sigma, \bar{z}) = (K_I, \sigma_I, \bar{s}_i)$ respectively.

Also, we derive the joint PDF of S_D and S_I, through the generation of two independent squared JFTS random variables, Z_1 and Z_2, and then using the transformation: $S_D = \rho Z_1 + \sqrt{1-\rho^2} Z_2$ and $S_I = Z_2$. Then, we need to find functions, $Z_1 = s_1(S_D, S_I)$ and $Z_2 = s_2(S_D, S_I)$, such that, $s_1(s_d, s_i) = \frac{s_d}{\rho} - \frac{s_i\sqrt{1-\rho^2}}{\rho}$ and $s_2(s_d, s_i) = s_i$. Next we calculate the Jacobian, $J = \det \begin{bmatrix} \frac{\partial s_1}{\partial s_d} & \frac{\partial s_1}{\partial s_i} \\ \frac{\partial s_2}{\partial s_d} & \frac{\partial s_2}{\partial s_i} \end{bmatrix} = 1$. The joint density of S_D and S_I is then given by,

$$\begin{aligned} &f_{S_D,S_I}(s_d, s_i) \\ &= |J| f(x_1, x_2) = f\big((s_d - s_i\sqrt{1-\rho^2})/\rho, s_i\big) \\ &= \sum_{j=1}^{4} D_{1j} \sum_{h=1}^{m} R_h^2\, e^{-D_2 - \frac{F_{1h}}{\rho}(s_d - s_i\sqrt{1-\rho^2}) - F_{2h}s_i} \Big[e^{B_{1j}+B_{2j}} \\ &\quad \times I_0\Big(4\sqrt{(s_d - s_i\sqrt{1-\rho^2})C_{1j}}\Big) I_0\big(4\sqrt{s_i C_{2j}}\big) + e^{B_{1j}-B_{2j}} \\ &\quad \times I_0\Big(4\sqrt{(s_d - s_i\sqrt{1-\rho^2})C_{1j}}\Big) I_0\big(4\sqrt{s_i C_{4j}}\big) + e^{-B_{1j}+B_{2j}} \\ &\quad \times I_0\Big(4\sqrt{(s_d - s_i\sqrt{1-\rho^2})C_{3j}}\Big) I_0\big(4\sqrt{s_i C_{2j}}\big) + e^{-B_{1j}-B_{2j}} \\ &\quad \times I_0\Big(4\sqrt{(s_d - s_i\sqrt{1-\rho^2})C_{3j}}\Big) I_0\big(4\sqrt{s_i C_{4j}}\big)\Big] \end{aligned} \quad (7)$$

where, $B_{1j} = \sigma_D\Delta T_j$, $B_{2j} = \sigma_I\Delta T_j$, $C_{1j} = K_D\sigma_D\hat{K}_D\hat{\sigma}_D(1-\Delta T_j)/(M_R\rho\bar{s}_d)$, $C_{2j} = K_I\sigma_I\hat{K}_I\hat{\sigma}_I(1-\Delta T_j)/(M_T\bar{s}_i)$, $C_{3j} = K_D\sigma_D\hat{K}_D\hat{\sigma}_D(1+\Delta T_j)/(M_R\rho\bar{s}_d)$, $C_{4j} = K_I\sigma_I\hat{K}_I\hat{\sigma}_I(1+\Delta T_j)/(M_T\bar{s}_i)$, $D_{1j} = b_j^2\hat{K}_D\hat{\sigma}_D\hat{K}_I\hat{\sigma}_I/(M_RM_T\bar{s}_d\bar{s}_i)$, $D_2 = K_D + \sigma_D + K_I + \sigma_I$, $F_{1h} = 1/2M_RP_2r_h^2$ and $F_{2h} = 1/2M_TP_2r_h^2$.

III. Outage Probability Analysis

The outage probability P_{out} is defined as the probability that the instantaneous SINR falls below a specified threshold ν_{th}, i.e., $P_{\text{out}} = \Pr\{\nu \le \nu_{\text{th}}\}$. This is equivalent to $P_{\text{out}} = \Pr\{\Psi \le N\nu_{\text{th}}\}$, where $\Psi = S_D - \nu_{\text{th}}S_I$. We denote the correlation coefficient between S_D and $\nu_{\text{th}} S_I$ by ρ_S. Here, we derive $P_{\text{out}} = \int_{-\infty}^{N\nu_{\text{th}}} f_{\Psi}(\psi)\mathrm{d}\psi = 1 - \int_{N\nu_{\text{th}}}^{\infty} f_{\Psi}(\psi)\mathrm{d}\psi$, where $f_{\Psi}(\psi)$ is the PDF of Ψ expressed as [8], [11] $f_{\Psi}(\psi) = f_{\Psi}(s_d - \nu_{\text{th}} s_i) = \int_{\max(0,\psi)}^{\infty} f_{S_D,\nu_{\text{th}} S_I}(\psi + \nu_{\text{th}} s_i, \nu_{\text{th}} s_i)\mathrm{d}s_i$, assuming that the interfering signal power will always be less than the desired signal power at the receiver,[2] i.e. $\Psi \geq 0$. The joint PDF of S_D and $\nu_{\text{th}} S_I$ in the above integrand can be obtained by replacing (s_i, ρ) with $(\nu_{\text{th}} s_i, \rho_S)$ in (7). The PDF of Ψ is given below for two cases separately.

- *Case I: $\psi = 0$:* In this case, using the infinite series expansion of modified Bessel function and integral solution from [12], we can have,

$$
\begin{aligned}
f_{\Psi}(\psi) &= \int_0^{\infty} f_{S_D,\nu_{\text{th}} S_I}(\psi + \nu_{\text{th}} s_i, \nu_{\text{th}} s_i)\mathrm{d}s_i \\
&= \sum_{j=1}^{4} D_{1j}\Omega_j \sum_{h=1}^{m} R_h^2\, e^{-D_2}\, e^{\frac{\psi W_{1h}}{2W_{2h}} - \psi\frac{F_{1h}}{\rho_S}} \sum_{u=0}^{\infty} \frac{4^u}{u!\sqrt{\pi}} \\
&\quad \times \mathsf{K}_{u+1/2}\big(\psi W_{1h}/2W_{2h}\big)\big(\psi/\nu_{\text{th}}^2 W_{1h} W_{2h}\big)^{u+1/2}
\end{aligned} \tag{9}
$$

  where $\mathsf{K}_{u+1/2}(g) = \sqrt{\frac{\pi}{2g}}\, e^{-g} \sum_{\upsilon=0}^{u} \frac{(u+\upsilon)!}{\upsilon!(u-\upsilon)!(2g)^{\upsilon}}$ is the $(u+1/2)$th-order modified Bessel function of the second kind [13], $\Omega_j = \Omega_{1j} + \Omega_{2j} + \Omega_{3j} + \Omega_{4j}$, $W_{1h} = F_{1h} + F_{2h}\rho_S - F_{1h}\sqrt{1-\rho_S{}^2}/\rho_S$, $W_{2h} = 1 - \sqrt{1-\rho_S{}^2}$, $\Omega_{1j} = e^{B_{1j}+B_{2j}} I_0\big(4\nu_{\text{th}}\sqrt{C_{1j}C_{2j}(1-\sqrt{1-\rho_S{}^2})}\big)$, $\Omega_{2j} = e^{B_{1j}-B_{2j}} I_0\big(4\nu_{\text{th}}\sqrt{C_{1j}C_{4j}(1-\sqrt{1-\rho_S{}^2})}\big)$, $\Omega_{3j} = e^{-B_{1j}+B_{2j}} I_0\big(4\nu_{\text{th}}\sqrt{C_{3j}C_{2j}(1-\sqrt{1-\rho_S{}^2})}\big)$ and $\Omega_{4j} = e^{-B_{1j}-B_{2j}} I_0\big(4\nu_{\text{th}}\sqrt{C_{3j}C_{4j}(1-\sqrt{1-\rho_S{}^2})}\big)$.
- *Case II: $\psi \neq 0$:* Similarly, in this case, using the integral solution from [12], we can have,

$$
\begin{aligned}
f_{\Psi}(\psi) &= \int_{\psi}^{\infty} f_{S_D,\nu_{\text{th}} S_I}(\psi + \nu_{\text{th}} s_i, \nu_{\text{th}} s_i)\mathrm{d}s_i \\
&= \sum_{j=1}^{4} D_{1j}\Omega_j \sum_{h=1}^{m} R_h^2 e^{-D_2} e^{\frac{\psi W_{1h}}{2W_{3h}} - \psi\frac{F_{1h}}{\rho_S}} \sum_{u=0}^{\infty} \frac{4^u}{u!\sqrt{\pi}} \\
&\quad \times \mathsf{K}_{u+1/2}\big(\psi W_{1h}/2W_{3h}\big)\big(\psi/\nu_{\text{th}}^2 W_{1h} W_{3h}\big)^{u+1/2}
\end{aligned} \tag{10}
$$

where $W_{3h} = \sqrt{1-\rho_S{}^2} - 1$. Solving the integral for ψ in (10), the final expression for P_{out} is given in (8), as shown at the bottom of this page, for $[-\pi < |\arg(\psi)| < \pi, \Re(F_{1h}) > 0, \Re(F_{2h}) > 0]$, where $\Re(\cdot)$ denotes the real part of its argument. Here $\Gamma(b,c)$ is the generalized upper incomplete Gamma function. As can be seen from (8), P_{out} depends on the JFTS shape parameter P_2 and the correlation coefficient ρ_S, the impact of which is numerically examined below. However, for our numerical analysis, we have truncated the infinite series representation of the outage probability at $u = 25$. Through trial and error, we found that with $u = 25$ we can approach an acceptable prediction of the outage probability.

[2]The interfering signal power will always be less than the desired signal power, as it consists of the delayed, down-scaled and correlated versions of the desired signal only.

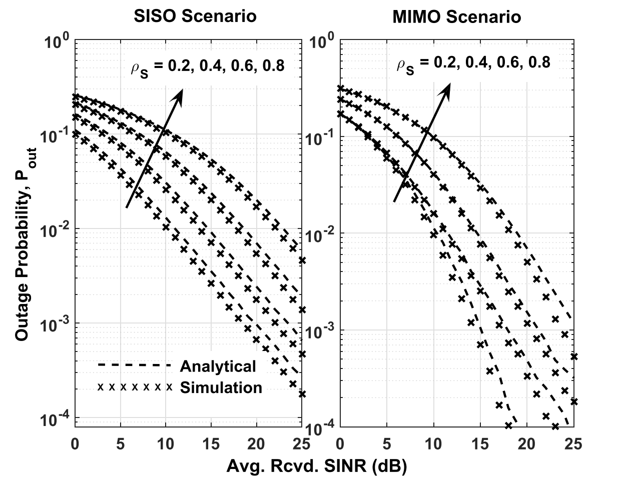

Fig. 1. P_{out} as a function of $\bar{s}_d/(\bar{s}_i + N)\nu_{\text{th}}$ with $\nu_{\text{th}} = 0$ dB, $N = -40$ dB, $\bar{s}_i = 10$ dB, $P_2 = 0.35$ over a JFTS link with varying ρ_S.

IV. Numerical Results and Discussion

We report the outage probability as a function of the average SINR per bit in the case of 16 Quadrature Amplitude Modulation (16 QAM), where the average received SINR per bit is defined as $\mathrm{E}\big\{S_D/((S_I+N)\nu_{\text{th}})\big\}E_b/N_0$, where E_b is the energy per bit and N_0 is the noise spectral density. We choose 16-QAM as our preferred modulation scheme since it can achieve the lower bound of outage probability in a moderately flat fading propagation environment. We compare the analytical results with those obtained through Monte Carlo simulation in order to validate the proposed analysis.

For simulation, the wireless communication channel between the transmit and the receive antennas is assumed to be suffering from AWGN and self-interference, and the composite fading / shadowing envelope is assumed to be JFTS distributed with statistically independent channel samples. For our analysis we have chosen the approximation index, $m = 20$ and we have set $\nu_{\text{th}} = 0$ dB.

Simulation results (Fig. 1 and Fig. 2) refer to both SISO ($M_T = 1$ and $M_R = 1$, single access point to a single mobile user communication) and MIMO ($M_T = 2$ and $M_R = 2$, full-duplex radios with multiple antennas for transmission and reception) scenarios.[3] In both cases, the analytical results offer a good agreement with the simulation results. However, in the

[3]In a MIMO system with M_T transmit and M_R receive antennas, the maximum achievable diversity order is equal to the total number of independent fading gains [15]. Hence, in order to exploit full diversity, we have assumed that the channel gain remains constant for a duration of l symbols i.e. $l \leq M_T + M_R - 1$ for our analysis.

$$
P_{\text{out}} = 1 - \Bigg[\sum_{j=1}^{4} D_{1j} \sum_{h=1}^{m} R_h^2 \sum_{u=0}^{\infty}\sum_{\upsilon=0}^{u} \frac{e^{-D_2}\Omega_j (u+\upsilon)!4^{u+\upsilon+1} W_{3h}}{2u!\upsilon!(u-\upsilon)!(W_{1h})^{u+\upsilon+1}\nu_{\text{th}}^{2u+1}} \Gamma\bigg(u-\upsilon+1, \frac{F_{2h} N\nu_{\text{th}}}{W_{3h}}\bigg)\Bigg]. \tag{8}
$$

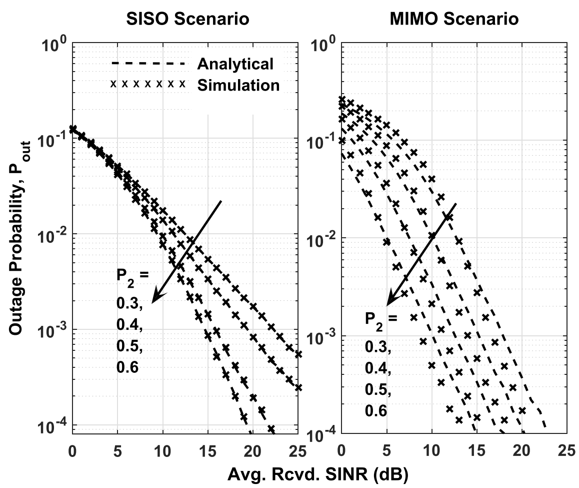

Fig. 2. P_{out} as a function of $\bar{s}_d/(\bar{s}_i + N)\nu_{\text{th}}$ with $\nu_{\text{th}} = 0$ dB, $N = -40$ dB, $\bar{s}_i = 10$ dB, $\rho_S = 0.3$ for over a JFTS link with varying P_2.

MIMO case, the analysis underestimates the outage probability for higher SINR. This can be the result of the truncation of the infinite series in (8) as trial and error method is not a perfect way to define a truncation bound. In that case we have to resort to methods similar to [14].

Fig. 1 demonstrates that P_{out} increases with ρ_S. It is worth highlighting that the results follow a trend exactly opposite of that in the Nakagami-*m* and Rayleigh fading cases, as shown in [1], where P_{out} decreases with the correlation coefficient between the desired and interfering signal powers. According to [1], this behavior is due to the fact that the impact of ρ_S decreases as the magnitude of $\bar{s}_i$ gets higher than N. The contrasting behavior exhibited in case of the JFTS distribution can be related to the fact that the higher the correlation between the desired and the interfering components, the more it becomes difficult for the receiver to correctly detect the desired signal components. Moreover, it is to be noted that JFTS distribution can never be expressed in terms of zero-mean complex Gaussian RVs. Therefore, $\bar{s}_i$ and N do not follow the same distribution (Gaussian) in case of JFTS, as in case of Nakagami-*m* distribution, where $\bar{s}_i$ and N are both zero-mean complex Gaussian.

Fig. 2 shows that P_{out} over a JFTS communication link in presence of self-interference decreases with the shape parameter, P_2. The parameter P_2 defines the mean-squared value of the scattered components in a composite JFTS faded/ shadowed channel and intuitively represents the variance of the shadowing distribution. If P_2 is increased, a large range of discrete shadowing values will be encountered over the path between the transmit and receive antennas. This will result in equal number of high and low main wave amplitudes thereby lowering the overall shadowing severity. In such a condition, performance improves with consequent reduction of outage probability over the JFTS faded /shadowed link.

On a final note, it is worth-mentioning that our numerical results are actually based on practical parameters observed in the detailed measurement campaign [6] on which the JFTS model characterization is based on. From [6], we have seen that the values of P_2 varies between 0.2 and 0.6 in a large office indoor wireless environment. That is the reason, we present outage probability results in Fig. 2 as a function of P_2 where P_2 is varied between 0.3 and 0.6. Similarly the values of $\bar{s}_d$ and $\bar{s}_i$ can be calculated from (2) to range between 7 dB and 13 dB for practical observed values of different JFTS parameters (K, σ). Hence, we choose the approximate mean values for $\bar{s}_d = 10$ dB and $\bar{s}_i = 10$ dB for our numerical analysis.

V. Conclusion

We have derived a mathematically tractable expression for the outage probability in the presence of self-interference over a JFTS fading/shadowing channel. In the derivation, we first obtain the PDF of squared JFTS variates and then the PDF of the difference between two correlated, not necessarily identically distributed, squared JFTS variates. Numerical results corroborated the analysis, and demonstrated that the outage probability in a self-interfering scenario increases with the increase in the correlation coefficient (ρ_S) and the decrease in the shape parameter (P_2).

References

[1] H. Holm and M. S. Alouini, "Sum and difference of two squared correlated Nakagami variates in connection with the McKay distribution," *IEEE Trans. Commun.*, vol. 52, no. 8, pp. 1367–1376, Aug. 2004.

[2] A. Ligeti, "Outage probability in the presence of correlated lognormal useful and interfering components," *IEEE Commun. Lett.*, vol. 4, no. 1, pp. 15–17, Jan. 2000.

[3] A. Ligeti and J. Zander, "Minimal cost coverage planning for single frequency networks," *IEEE Trans. Broadcast.*, vol. 45, no. 1, pp. 78–87, Mar. 1999.

[4] A. Bazzi, B. M. Masini, and A. Zanella, "Performance analysis of V2V beaconing using LTE in direct mode with full duplex radios," *IEEE Wireless Commun. Lett.*, vol. 4, no. 6, pp. 685–688, Dec. 2015.

[5] V. Syrjala, M. Valkama, L. Anttila, T. Riihonen, and D. Korpi, "Analysis of oscillator phase-noise effects on self-interference cancellation in full-duplex OFDM radio transceivers," *IEEE Wireless Commun. Lett.*, vol. 13, no. 6, pp. 2977–2990, Jun. 2014.

[6] I. Dey, G. G. Messier, and S. Magierowski, "Joint fading and shadowing model for large office indoor WLAN environments," *IEEE Trans. Antennas Propag.*, vol. 62, no. 4, pp. 2209–2222, Apr. 2014.

[7] I. Dey, G. G. Messier, and S. Magierowski, "Fading statistics for the joint fading and two path shadowing channel," *IEEE Wireless Commun. Lett.*, vol. 3, no. 3, pp. 301–304, Jun. 2014.

[8] A. Papoulis and S. U. Pillai, *Probability, Random Variables Stochastic Processes*, 2nd ed. New York. NY, USA: McGraw Hill, 1984.

[9] Y.-S. Choi and H.-S. Mehr, "Simultaneous transmission and reception: Algorithm, design and system level performance," *IEEE Trans. Wireless Commun.*, vol. 12, no. 12, pp. 5992–6010, Dec. 2013.

[10] M. Duarte *et al.*, "Design and characterization of a full-duplex multi-antenna system for WiFi networks," *IEEE Trans. Veh. Technol.*, vol. 63, no. 3, pp. 1160–1177, Mar. 2014.

[11] S. Nadarajah, "A review of results on sums of random variables," *Acta Appl. Math.*, vol. 103, no. 2, pp. 131–140, Sep. 2008.

[12] I. S. Gradshteyn and I. M. Ryzhik, *Table of Integrals, Series and Products*, 7th ed. New York, NY, USA: Academic, 2007.

[13] M. Abramowitz and I. A. Stegun, *Handbook of Mathematical Functions, With Formulas, Graphs, and Mathematical Tables*, 9th ed. New York, NY, USA: Dover, 1972.

[14] I. Dey, T. Tsiftsis, and C. Rowell, "Achievable channel cut-off rate and bandwidth efficiency in indoor wireless environments," *IEEE Trans. Veh. Technol.*, to be published, doi: 10.1109/TVT.2016.2553358.

[15] L. Zheng and D. N. C. Tse, "Diversity and multiplexing: A fundamental tradeoff in multiple-antenna channels," *IEEE Trans. Inf. Theory*, vol. 49, no. 5, pp. 1073–1096, May 2003.